

# Changes in the Tropical Pacific SST Trend from CMIP3 to CMIP5 and Its Implication of ENSO\*

SANG-WOOK YEH

*Department of Environmental Marine Science, Hanyang University, Ansan, South Korea*

YOO-GEUN HAM

*Global Modeling and Assimilation Office, NASA Goddard Space Flight Center, Greenbelt,  
and Goddard Earth Sciences Technology and Research Studies and Investigations,  
Universities Space Research Association, Columbia, Maryland*

JUNE-YI LEE

*Department of Meteorology, and International Pacific Research Center, University of Hawaii at Manoa, Honolulu, Hawaii*

(Manuscript received 15 May 2012, in final form 23 July 2012)

## ABSTRACT

This study assesses the changes in the tropical Pacific Ocean sea surface temperature (SST) trend and ENSO amplitude by comparing a historical run of the World Climate Research Programme Coupled Model Intercomparison Project (CMIP) phase-5 multimodel ensemble dataset (CMIP5) and the CMIP phase-3 dataset (CMIP3). The results indicate that the magnitude of the SST trend in the tropical Pacific basin has been significantly reduced from CMIP3 to CMIP5, which may be associated with the overestimation of the response to natural forcing and aerosols by including Earth system models in CMIP5. Moreover, the patterns of tropical warming over the second half of the twentieth century have changed from a La Niña-like structure in CMIP3 to an El Niño-like structure in CMIP5. Further analysis indicates that such changes in the background state of the tropical Pacific and an increase in the sensitivity of the atmospheric response to the SST changes in the eastern tropical Pacific have influenced the ENSO properties. In particular, the ratio of the SST anomaly variance in the eastern and western tropical Pacific increased from CMIP3 to CMIP5, indicating that a center of action associated with the ENSO amplitude has shifted to the east.

## 1. Introduction

The El Niño–Southern Oscillation (ENSO) is the most prominent interannual variability on Earth. Changes in the amplitude and frequency of ENSO can affect the occurrence of climate extremes around the globe (McPhaden et al. 2006).

In 2007, the Intergovernmental Panel on Climate Change (IPCC) released its Fourth Assessment Report (Solomon et al. 2007), which concludes that the warming

of Earth is unequivocal. Furthermore, recent studies have shown that global warming may significantly influence ENSO properties by altering the background state of the tropical Pacific Ocean (Timmermann et al. 1999; Fedorov and Philander 2000; Koutavas et al. 2002; Li et al. 2011). Hence, subtle patterns of evolving tropical Pacific sea surface temperatures (SSTs) induced by global warming could have a disproportionate effect on the climate in many regions of the world (Xie et al. 2010; Shin and Sardeshmukh 2011). Therefore, it is crucial to correctly simulate the structure of changes in the ocean SST in response to external forcings to understand the changes in ENSO properties. Consequently, this issue has been thoroughly examined using the World Climate Research Programme's (WCRP) Coupled Model Intercomparison Project phase-3 (CMIP3) multimodel database (Meehl et al. 2007); yet, despite such efforts, there is little agreement in

---

\* School of Ocean and Earth Science and Technology Publication Number 8717 and International Pacific Research Center Publication Number 902.

---

*Corresponding author address:* Yoo-Geun Ham, Goddard Space Flight Center, Mail Code 610.1, Greenbelt, MD 20771.  
E-mail: yoo-geun.ham@nasa.gov

TABLE 1. The observed difference [ $^{\circ}\text{C} (100 \text{ yr})^{-1}$ ] in the trends between the western tropical Pacific (WP;  $5^{\circ}\text{N}$ – $5^{\circ}\text{S}$ ,  $120^{\circ}\text{E}$ – $170^{\circ}\text{W}$ ) and the eastern tropical Pacific (EP;  $5^{\circ}\text{N}$ – $5^{\circ}\text{S}$ ,  $150^{\circ}$ – $90^{\circ}\text{W}$ ) from 1950 to 2010.

SST dataset	Obs WP – EP trend
Hadley SST	0.69
ERSST V3	0.06
Kaplan SST	0.15
ECMWF ORA3	0.80

the climate community as to whether the structure of the mean SST changes is trending toward an El Niño-like pattern or a La Niña-like pattern under the global warming (Collins 2005; Collins et al. 2010; Vecchi et al. 2008). In addition, it is still not clear whether the ENSO amplitude has been enhanced, has been reduced, or has not altered significantly under these mean state changes.

Likewise, observations in the ocean SST with a period of more than 100 yr indicate a diversity of structural changes (Deser et al. 2010). For example, a warming trend with an El Niño-like pattern has been identified during recent decades (Graham 1995; Trenberth and Hoar 1996), but some evidence suggests that the zonal SST gradient across the tropical Pacific has increased (Cane et al. 1997; Karnauskas et al. 2009; An et al. 2012). Despite this information, some results consistently indicate that the linear trend in the western tropical Pacific is larger than that in the eastern tropical Pacific for the second half of the twentieth century. Table 1 shows the average linear trend in the western tropical Pacific ( $5^{\circ}\text{N}$ – $5^{\circ}\text{S}$ ,  $120^{\circ}\text{E}$ – $170^{\circ}\text{W}$ ) and in the eastern tropical Pacific ( $5^{\circ}\text{N}$ – $5^{\circ}\text{S}$ ,  $150^{\circ}$ – $90^{\circ}\text{W}$ ) for the period of 1950–2010 from the various observed SST datasets. Clearly, the linear trend in the western Pacific is larger than that in the eastern Pacific in all SST datasets, indicating that the zonal SST gradient across the tropical Pacific has become strong. Consequently, since the WCRP CMIP5 (phase 5) multimodel ensemble datasets (Taylor et al. 2012) have recently been released, it is useful to compare the structure of the tropical Pacific SST changes during a similar time period (i.e., after 1950) using the CMIP3 and CMIP5 datasets. Furthermore, it is interesting to examine how changes in the ocean SST structure under global warming from CMIP3 to CMIP5 may be associated with changes in the ENSO amplitude.

Thus, the intent of this paper is to compare the SST trends from the tropical Pacific using CMIP3 coupled general circulation models (CGCMs) and CMIP5 CGCMs and to examine how such changes in SST trends are associated with changes in the ENSO amplitude. We directly

compare CMIP3 CGCMs with CMIP5 CGCMs, noting that the CMIP5 CGCMs have been improved from the CMIP3 CGCMs, following the recommended CMIP5 specifications (online at <http://cmip-pcmdi.llnl.gov/cmip5/forcing.html>).

## 2. Data and method

The observed SST information used in Table 1 are from the Hadley Centre Global Sea Ice and Sea Surface Temperature (HadISST) dataset (Rayner et al. 2003); the extended reconstruction SST, version 3 (ERSST V3), dataset (Smith and Reynolds 2004); the National Oceanic and Atmospheric Administration (NOAA) Climate Diagnostic Center dataset known as the Kaplan SST dataset (Kaplan et al. 1998); and the European Centre for Medium-Range Weather Forecasts (ECMWF) Ocean Reanalysis, version S3 (ORA-3), SST dataset (Balmaseda et al. 2008).

We use 12 CGCM simulations selected from a historical run (i.e., from a twentieth-century run) that have SST datasets from both the CMIP3 and CMIP5 multimodel databases. Table 2 shows the official CMIP3 and CMIP5 model names for each modeling center. Some CMIP5 CGCMs are specified as Earth system models (e.g., CanESM2, GFDL-ESM2G, HadGEM2-CC, HadGEM2-ES, and MIROC-ESM; note that all model and institution acronyms referred to anywhere in the text are defined fully in the footnote material to Table 2), which respond to specific time-varying concentrations of various atmospheric constituents such as greenhouse gases and other components of the atmosphere, ocean, and sea ice. These models are coupled to biogeochemical components, which account for the exchange of carbon among the ocean, atmosphere, and terrestrial biosphere carbon reservoirs. Additionally, in some simulations, these models may incorporate components such as interactive prognostic aerosols, chemical elements, and dynamic vegetation (Taylor et al. 2012). For example, CanESM2 is the latest-generation Canadian CGCM that originated from the Canadian Centre for Climate Modelling and Analysis (CCCma) CGCM3.1 (T63) model in CMIP3, and it includes an interactive carbon cycle, an interactive sulfur cycle, and the effect of a sulfate aerosol on cloud brightness (Gillett et al. 2012). Furthermore, it is recognized that some CMIP5 CGCMs perform simulations with a higher resolution or a more complete treatment of the atmospheric chemistry than is done for CMIP3 CGCMs. Hence, detailed explanations for each CGCM can be found online (at [http://cmip-pcmdi.llnl.gov/cmip5/experiment\\_design.html](http://cmip-pcmdi.llnl.gov/cmip5/experiment_design.html)) as well as in various related papers (Taylor et al. 2009, 2012).

TABLE 2. Model institutions and descriptions, as specified in CMIP, used in this study.

Modeling center*	Model No.	CMIP3 model name**	CMIP5 model name**
CCCma	1	CGCM3.1(T63)	CanESM2
NCAR	2	CCSM3	CCSM4
CNRM-CERFACS	3	CNRM-CM3	CNRM-CM5
CSIRO-QCCCE	4	CSIRO-Mk3.5	CSIRO-Mk3.6.0
LASG/IAP; LASG-CESS	5	FGOALS-g1.0	FGOALS-g2
NOAA GFDL	6	GFDL-CM2.1	GFDL-ESM2G
MOHC	7	UKMO-HadCM3	HadGEM2-CC
MOHC	8	UKMO-HadGEM1	HadGEM2-ES
INM	9	INM-CM3.0	INM-CM4
IPSL	10	IPSL-CM4	IPSL-CM5A-LR
MIROC	11	MIROC3.2(hires)	MIROC-ESM
MRI	12	MRI-CGCM2.3.2a	MRI-CGCM3

\* Institutional acronyms: CCCma—Canadian Centre for Climate Modelling and Analysis; NCAR—National Center for Atmospheric Research; CNRM—Météo-France/Centre National de Recherches Météorologiques (CMIP3) and CNRM-CERFACS—Centre Européen de Recherche et Formation Avancées en Calcul Scientifique (CMIP5); CSIRO—Commonwealth Scientific and Industrial Research Organisation Advanced Research (CMIP3) and CSIRO-QCCCE—CSIRO in collaboration with Queensland Climate Change Centre of Excellence (CMIP5); LASG/IAP—State Key Laboratory of Numerical Modeling for Atmospheric Sciences and Geophysical Fluid Dynamics, of the Institute of Atmospheric Physics (CMIP3); LASG-CESS—LASG/IAP, Chinese Academy of Sciences and Center for Earth System Science, Tsinghua University (CMIP5); NOAA GFDL—Geophysical Fluid Dynamics Laboratory; MOHC—Met Office Hadley Centre (CMIP5) for Climate Prediction and Research (CMIP3); INM—Institute of Numerical Mathematics; IPSL—L'Institut Pierre-Simon Laplace; MIROC—Center for Climate System Research of the University of Tokyo, National Institute for Environmental Studies, and Frontier Research Center for Global Climate Change of the Japan Agency for Marine-Earth Science and Technology (JAMSTEC) (CMIP3) and JAMSTEC, Atmosphere and Ocean Research Institute of the University of Tokyo, and National Institute for Environmental Studies (CMIP5); MRI—Meteorological Research Institute.

\*\* Model names: CGCM3.1(T63)—third-generation Coupled Global Climate Model with T-63 spectral resolution; CanESM2—second-generation Canadian Earth System Model; CCSM3/4—Community Climate System Model, versions 3 and 4; CM3/5—Coupled Global Climate Model, versions 3 and 5; Mk3.5/3.6.0—Mark 3.5 and 3.6.0; FGOALS-g1.0/2—Flexible Global Ocean-Atmosphere-Land System Model, gridpoint versions 1.0 and 2; CM2.1—Climate Model, version 2.1; ESM2G—Earth System Model using the Generalized Ocean Layer Dynamics code base; UKMO-HadCM3—third climate configuration of the Met Office Hadley Centre Unified Model; UKMO-HadGEM1—Met Office Hadley Centre Global Environmental Model, version 1; HadGEM2-CC/ES—Hadley Centre Global Environmental Model, version 2, with Carbon Cycle/Earth System configurations (CC has troposphere, land surface and hydrology, aerosols, ocean and sea-ice, terrestrial carbon cycle, and ocean biogeochemistry; ES has all that plus chemistry); CM3.0/4—Coupled Model, versions 3 and 4; CM4/5A-LR—Climate Model, version 4 and version 5A (same physics as version 4) in low-resolution configuration; MIROC3.2(hires)/-ESM—Model for Interdisciplinary Research on Climate, version 3.2 with high resolution and Earth System Model version; CGCM2.3.2a/3—Coupled General Circulation Model, versions 2.3.2a and 3.

### 3. Results

To illustrate the response of tropical Pacific SST patterns to global warming over the second half of the twentieth century, specifically highlighting the difference between CMIP3 and CMIP5, Figs. 1a and 1b display the ensemble-averaged linear trends simulated by the historical run of 12 CMIP3 and CMIP5 CGCMs, respectively, for the period of 1950–2000.

The simulation of the CMIP3 CGCM (Fig. 1a) exhibits a maximum SST trend in the central tropical/off-equatorial Pacific region. The central Pacific Ocean is projected to experience the greatest amount of warming, whereas the southeastern Pacific Ocean is expected to warm less. Interestingly, this expectation is largely consistent with the observed spatial pattern of SST change over the beginning of the twenty-first century, which is averaged over 22 CMIP3 CGCMs under a midrange

emission scenario (IPCC Special Report on Emission Scenarios A1B; see Fig. 1 in Clement et al. 2010). Moreover, although the overall pattern of linear trends in the CMIP3 deviates from the observations in some regions (not shown here), it is consistent that the SST trend in the western tropical Pacific is larger than that in the eastern tropical Pacific, indicating that zonal SST gradient across the tropical Pacific has become strong during the second half of the twentieth century.

It is striking, then, that the magnitude of the linear trend of SSTs in the tropical Pacific basin is reduced significantly in the CMIP5 (Fig. 1b) when compared with the CMIP3 (Fig. 1a). Whereas the linear trend of the CMIP3 is around 1.0°–1.2°C in the western and central tropical Pacific, it is around 0.4°–0.6°C for the CMIP5. Furthermore, it is not clear why this reduction occurred, particularly because the CMIP3 and CMIP5 datasets were acquired during the same historical period.

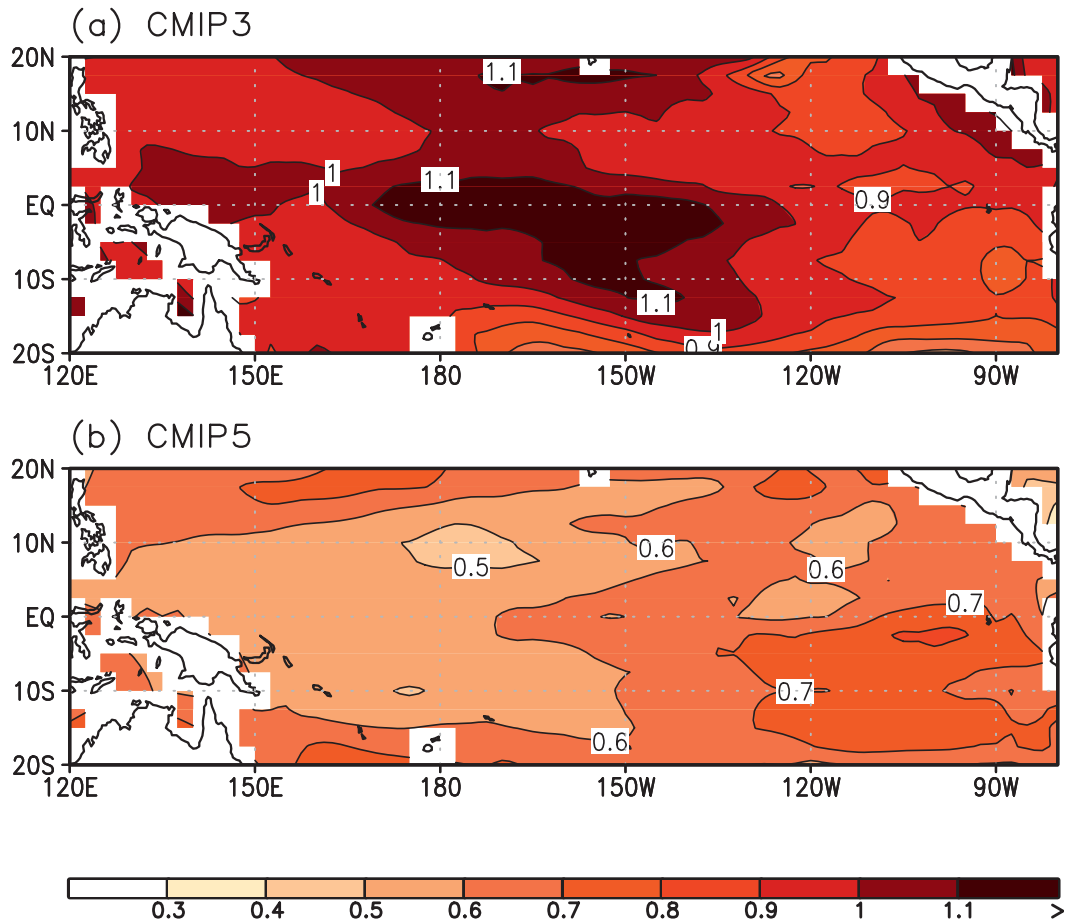


FIG. 1. The linear trends of SSTA [ $^{\circ}\text{C} (100 \text{ yr})^{-1}$ ] from 1950 to 2000 in (a) the CMIP3 MME and (b) the CMIP5 MME.

However, it is possible that the CMIP5, which includes some CGCMs with an Earth system model component, overestimates the response to natural forcings and aerosols. In a previous study (Gillett et al. 2012), for example, a relatively low and tightly constrained estimate of the transient climate response and relatively low projections of twenty-first-century warming under the representative concentration pathway are simulated using CMIP5 CanESM2, which employed an Earth system model component from CMIP3 CCCma CGCM3.1 (T63). This result prompts the need to examine additional models and the detailed physical processes within them to identify the changes from CMIP3 to CMIP5. Ideally, these studies would also better account for the use of various Earth system model components.

Figure 1 also indicates that the location of the maximum SST trend has shifted to the east from CMIP3 to CMIP5, resulting in a warming trend in the eastern tropical Pacific that is larger than that in the western tropical Pacific in CMIP5. The multimodel ensemble

(MME) difference of the trend over the western Pacific ( $5^{\circ}\text{N}$ – $5^{\circ}\text{S}$ ,  $120^{\circ}\text{E}$ – $170^{\circ}\text{W}$ ) from that in the eastern Pacific ( $5^{\circ}\text{N}$ – $5^{\circ}\text{S}$ ,  $150^{\circ}$ – $90^{\circ}\text{W}$ ) is  $-0.11^{\circ}\text{C} (100 \text{ yr})^{-1}$ , whereas that in CMIP3 is  $0.07^{\circ}\text{C} (100 \text{ yr})^{-1}$ . This shift suggests that the zonal SST gradient across the tropical Pacific has become weak in CMIP5. Note that this value in CMIP3 becomes weakly positive with recent 30-yr output [i.e.,  $0.15^{\circ}\text{C} (100 \text{ yr})^{-1}$ ], whereas the La Niña-like trend is robust during these decades in observations. However, the value is still smaller than that in CMIP5 [i.e.,  $0.41^{\circ}\text{C} (100 \text{ yr})^{-1}$ ], implying that the trend in CMIP3 is closer to the observed one than is that in CMIP5, even though there are systematic errors in simulating global warming trends in both CMIP archives.

One can ask why there is systematic error in simulating La Niña-like trends in CMIP archives. It might be due to the bias in the climate models in the tropical Pacific. Recently, An et al. (2012) argued that there are two competing processes to determine the trend over the

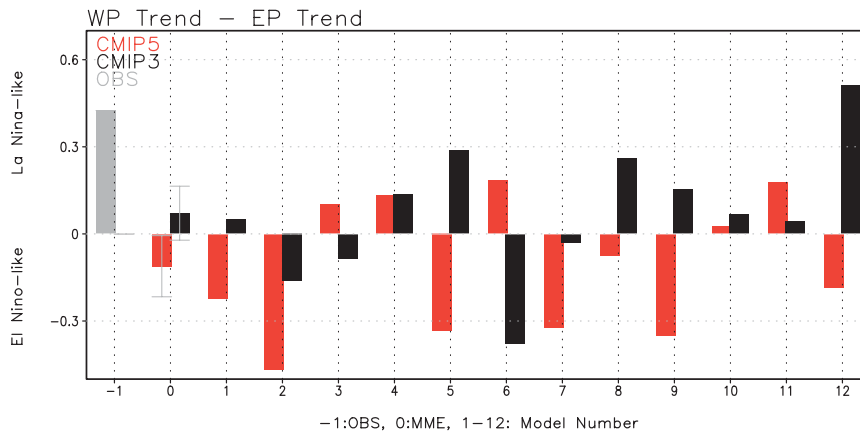


FIG. 2. The difference of trends over the western Pacific from that over the eastern Pacific from 1950 to 2000 [ $^{\circ}\text{C} (100 \text{ yr})^{-1}$ ]. The positive value indicates that the western Pacific trend is greater than the eastern Pacific trend (La Niña-like). Note that -1 on the x axis denotes the ensemble mean from the four different SST datasets in observations and 0 denotes the MME from the CMIP3 (black bar) and the CMIP5 (red bar), and each number from 1 to 12 denotes the corresponding climate model shown in Table 2. The gray error bars for MME denote the 90% confidence level using the standard deviation (STD) of ratio values among CMIP models.

eastern Pacific (i.e., a cooling effect from evaporative cooling and a warming effect from vertical thermal advection), and there is a possibility that the warming effect is excessively simulated, especially in CMIP5 models. In addition, there is a possibility that the trend signal over the recent decade is mixed up with the decadal variability over the Pacific (i.e., Pacific decadal oscillation; Mantua et al. 1997). On the other hand, some studies pointed out that there is a linkage between the Atlantic and the Pacific on a decadal time scale and that the La Niña-like signal over the tropical Pacific in recent decades is partly originated from the decadal variability over the Atlantic (Kucharski et al. 2011). Because the decadal variability in a twentieth-century run is not in phase with the observed one because of the lack of an initialization process, this may be the reason for different temperature change between the model and observations. Further analysis should be performed within this line of reasoning.

To examine similar structural changes in the SST trend from CMIP3 to CMIP5 in more detail, Fig. 2 displays the east–west trend difference (i.e., the western tropical Pacific minus the eastern tropical Pacific) for each CGCM, as well as their ensemble means and the observation. Note that the east–west trend difference in the observation is based on the four different SST datasets shown in Table 1. If the trend difference is above (below) zero, it represents a La Niña-like (El Niño-like) structure of the SST trend over the second half of the twentieth century, indicating that warming in the western (eastern) tropical Pacific is more dominant than that

in the eastern (western) tropical Pacific. The ensemble mean, which is denoted in the left-hand side of Fig. 2, indicates that the patterns of tropical warming over the second half of the twentieth century have significantly changed from a La Niña-like structure in CMIP3 to an El Niño-like structure in CMIP5. Whereas 8 of the 12 patterns represent a La Niña-like structure of the SST trend in CMIP3, 5 of the 12 do so in CMIP5. Except for 3 CGCMs [i.e., CNRM-CM3, GFDL-CM2.1, and MIROC3.2(hires)], the other 9 CGCMs show an east–west trend difference that has been reduced from CMIP3 to CMIP5. Among them, the sign of the east–west trend difference has changed in five CGCMs [i.e., the CCCma CGCM3.1(T63), FGOALS-g1.0, UKMO-HadGEM1, INM-CM3.0, and MRI-CGCM2.3.2a].

One can expect that such changes may influence the ENSO properties for both the CMIP3 and CMIP5 because the background state of the tropical Pacific has evolved between the two databases. In particular, this study focuses on the shift in an SST center of action associated with the ENSO amplitude, which is known to have changed significantly because of the mean state change (Yeh et al. 2009). To illustrate this effect, Fig. 3 displays the ratios of SSTA variance in the eastern tropical Pacific (i.e., the Niño-3 region:  $5^{\circ}\text{N}$ – $5^{\circ}\text{S}$ ,  $150^{\circ}$ – $90^{\circ}\text{W}$ ) to that in the western tropical Pacific (the Niño-4 region:  $5^{\circ}\text{N}$ – $5^{\circ}\text{S}$ ,  $160^{\circ}\text{E}$ – $150^{\circ}\text{W}$ ) from CMIP3 to CMIP5. It also displays their ensemble means and the observation. Note that an increase in this ratio indicates that a center of action associated with an ENSO amplitude has shifted to the east from CMIP3 to CMIP5. This

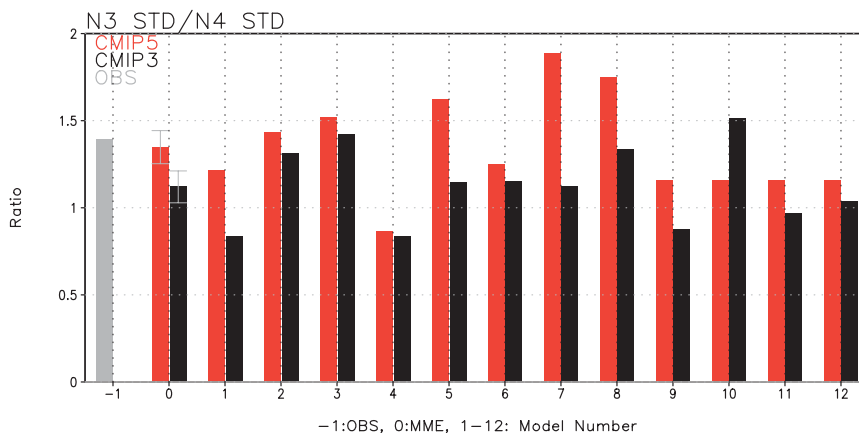


FIG. 3. As in Fig. 2, but for the ratio of the STD of the Niño-3 index to that of the Niño-4 index from CMIP5 (red bars) and CMIP3 (black bars) models during 1950–2000.

SSTA variance is calculated after removing the linear trend since it is to measure the interannual variability. Overall, the ratio of the SSTA variances increases from CMIP3 to CMIP5 as seen from the comparison of the ensemble-mean ratios. Furthermore, the increase in the SSTA variance ratio of the aforementioned five CGCMs, for which the sign of the east–west trend difference switched from CMIP3 to CMIP5, is more prominent. That is, the ensemble-mean ratio in the five CGCMs increases from CMIP3 (1.03) to CMIP5 (1.38).

Changes in the spatial patterns of tropical warming can induce a change in the ratio of the SSTA variance in the eastern and western tropical Pacific from CMIP3 to CMIP5. In other words, a greater amount of warming in the eastern tropical Pacific relative to the western tropical Pacific in CMIP5 (i.e., an El Niño–like structure of the SST trend) can amplify the SSTA variability in the eastern tropical Pacific through enhanced air–sea coupled processes (Choi et al. 2009). To measure the air–sea coupling strength over the eastern tropical Pacific, Fig. 4 displays the ensemble-mean regression coefficients between the mean SST and the mean precipitation over the Niño-3 region for 12 CMIP3 and CMIP5 CGCMs. An increase in this regression coefficient indicates that the atmospheric response to ocean SST changes has become more sensitive in the eastern tropical Pacific. Moreover, these coefficients systematically increase in CMIP5, suggesting an enhanced SSTA variance in the eastern tropical Pacific in CMIP5. Consequently, this study posits that both an El Niño–like structure of the SST trend and an increase in the sensitivity of the atmospheric response to SST changes in the eastern tropical Pacific from CMIP3 to CMIP5 may contribute to enhancing the ratio of the SSTA variance in the eastern and western tropical Pacific regions.

#### 4. Summary and discussion

Various observational data sources present discrepancies among their SST trends in the tropical Pacific throughout the twentieth century (Deser et al. 2010). Nevertheless, the four SST datasets used in this study indicate that the linear trend in the western Pacific is larger than that in the eastern Pacific in all SST datasets, suggesting that a zonal SST gradient across the tropical Pacific has become strong over the second half of the twentieth century (1950–2010). To verify this effect, the CMIP3 and CMIP5 multimodel datasets were utilized to simulate the tropical Pacific SST trends throughout a historical run from 1950 to 2000. It was found that the magnitude of the linear trend of the SST in the tropical Pacific basin decreased significantly from CMIP3 to CMIP5, which might be associated with the inclusion of an Earth system model component in the CMIP5 dataset. The patterns of tropical warming over the second half of the twentieth century evolve from a La Niña–like structure in CMIP3 to an El Niño–like structure in CMIP5. Such changes influence the ENSO properties in these two datasets by altering the background state of the tropical Pacific. In particular, the ratio of the SSTA variance in the eastern and western tropical Pacific was found to have increased from CMIP3 to CMIP5, indicating that a center of action associated with the ENSO amplitude had shifted to the east for CMIP5.

Consequently, we contend that both an El Niño–like structure of the SST trend and an increase in the sensitivity of the atmospheric response to SST changes in the eastern tropical Pacific from CMIP3 to CMIP5 contribute to an enhanced ratio of the SSTA variance in the eastern and western tropical Pacific regions. Yet, we do not exclude the possibility that an increase in the

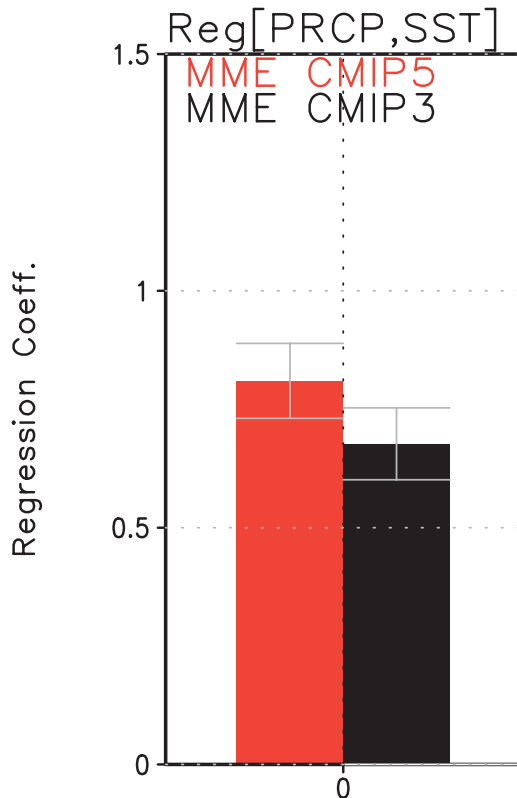


FIG. 4. The MME of precipitation regression coefficients over the Niño-3 region with respect to the Niño-3 SSTA ( $\text{mm day}^{-1} \text{ } ^\circ\text{C}^{-1}$ ) during 1950–2000 using CMIP3 (black bar) and CMIP5 (red bar) CGCMs. The gray error bars denote 90% confidence level using the STD of ratio values among CMIP models.

sensitivity of the atmospheric response to SST changes in the eastern tropical Pacific could cause a change in the tropical SST trend pattern from CMIP3 to CMIP5. In other words, an increase in the coupled air–sea process in the eastern tropical Pacific may be able to enhance the ratio of the SSTA variance between the eastern and western tropical Pacific regions. Then, this enhanced SSTA variance could induce a change in the tropical Pacific background state toward an El Niño-like structure via a nonlinear mechanism (Timmermann 2003; Rodgers et al. 2004; Yeh and Kirtman 2004).

**Acknowledgments.** We acknowledge the WCRP's Working Group on Coupled Modeling, which is responsible for CMIP, and we thank the climate modeling groups (listed in Table 2) for producing and making available their model output. For CMIP, the U.S. Department of Energy's Program for Climate Model Diagnosis and Intercomparison provides coordinating support and led development of software infrastructure in partnership with the Global Organization for Earth System Science Portals. S.-W. Yeh was funded by the

Korea Meteorological Administration Research and Development Program under Grant CATER 2012–3041. J.-Y. Lee acknowledges support from the International Pacific Research Center (IPRC) which is funded jointly by JAMSTEC, NOAA, and NASA.

#### REFERENCES

- An, S.-I., J.-W. Kim, S.-H. Im, B.-M. Kim, and J.-H. Park, 2012: Recent and future sea surface temperature trends in tropical Pacific warm pool and cold tongue regions. *Climate Dyn.*, **39**, 1373–1383, doi:10.1007/s00382-011-1129-7.
- Balmaseda, M. A., A. Vidard, and D. L. T. Anderson, 2008: The ECMWF Ocean Analysis System: ORA-S3. *Mon. Wea. Rev.*, **136**, 3018–3034.
- Cane, M., A. C. Clement, A. Kaplan, Y. Kushnir, D. Pozdnyakov, R. Seager, S. E. Zebiak, and R. Murtugudde, 1997: Twentieth-century sea surface temperature trends. *Science*, **275**, 957–960, doi:10.1126/science.275.5302.957.
- Choi, J., S.-I. An, B. Dewitte, and W. W. Hsieh, 2009: Interactive feedback between the tropical Pacific decadal oscillation and ENSO in a coupled general circulation model. *J. Climate*, **22**, 6597–6611.
- Clement, A. C., A. C. Baker, and J. Leloup, 2010: Climate change: Patterns of tropical warming. *Nat. Geosci.*, **3**, 8–9.
- Collins, M., 2005: El Niño- or La Niña-like climate change? *Climate Dyn.*, **24**, 89–104.
- , and Coauthors, 2010: The impact of global warming on the tropical Pacific Ocean and El Niño. *Nat. Geosci.*, **3**, 391–397.
- Deser, C., A. S. Phillips, and M. A. Alexander, 2010: Twentieth century tropical sea surface temperature trends revisited. *Geophys. Res. Lett.*, **37**, L10701, doi:10.1029/2010GL043321.
- Fedorov, A. V., and S. G. H. Philander, 2000: Is El Niño changing? *Science*, **288**, 1997–2002.
- Gillett, N. P., V. K. Arora, G. M. Flato, J. F. Scinocca, and K. von Salzen, 2012: Improved constraints on 21st-century warming derived using 160 years of temperature observations. *Geophys. Res. Lett.*, **39**, L01704, doi:10.1029/2011GL050226.
- Graham, N. E., 1995: Simulations of recent global temperature trends. *Science*, **267**, 666–671.
- Kaplan, A., M. A. Cane, Y. Kushnir, A. C. Clement, M. B. Blumenthal, and B. Rajagopalan, 1998: Analyses of global sea surface temperature 1856–1991. *J. Geophys. Res.*, **103**, 18 567–18 589.
- Karnauskas, K., R. Seager, A. Kaplan, Y. Kushnir, and M. A. Cane, 2009: Observed strengthening of the zonal sea surface temperature gradient across the equatorial Pacific Ocean. *J. Climate*, **22**, 4316–4321.
- Koutavas, A., J. Lynch-Stieglitz, T. M. Marchitto Jr., and J. P. Sachs, 2002: El Niño-like pattern in ice age tropical Pacific sea temperature. *Science*, **297**, 226–230.
- Kucharski, F., I.-S. Kang, R. Farneti, and L. Feudale, 2011: Tropical Pacific response to 20th century Atlantic warming. *Geophys. Res. Lett.*, **38**, L03702, doi:10.1029/2010GL046248.
- Li, J., S.-P. Xie, E. R. Cook, G. Huang, R. D'Arrigo, F. Liu, J. Ma, and X.-T. Zheng, 2011: Interdecadal modulation of El Niño amplitude during the past millennium. *Nat. Climate Change*, **1**, 114–118.
- Mantua, N. J., S. R. Hare, Y. Zhang, J. M. Wallace, and R. C. Francis, 1997: A Pacific interdecadal climate oscillation with impacts on salmon production. *Bull. Amer. Meteor. Soc.*, **78**, 1069–1079.

- McPhaden, M. J., S. E. Zebiak, and M. H. Glantz, 2006: ENSO as an integrating concept in Earth science. *Science*, **314**, 1740–1745.
- Meehl, G. A., C. Covey, T. Delworth, M. Latif, B. McAvaney, J. F. B. Mitchell, R. J. Stouffer, and K. E. Taylor, 2007: The WCRP CMIP3 multimodel dataset: A new era in climate change research. *Bull. Amer. Meteor. Soc.*, **88**, 1383–1394.
- Rayner, N., D. E. Parker, E. B. Horton, C. K. Folland, L. V. Alexander, D. P. Rowell, E. C. Kent, and A. Kaplan, 2003: Global analyses of sea surface temperature, sea ice, and night marine air temperature since the late nineteenth century. *J. Geophys. Res.*, **108**, 4407, doi:10.1029/2002JD002670.
- Rodgers, K. B., P. Friederichs, and M. Latif, 2004: Tropical Pacific decadal variability and its relation to decadal modulations of ENSO. *J. Climate*, **17**, 3761–3774.
- Shin, S.-I., and P. D. Sardeshmukh, 2011: Critical influence of the pattern of tropical ocean warming on remote climate trends. *Climate Dyn.*, **36**, 1577–1591.
- Smith, T. M., and R. W. Reynolds, 2004: Improved extended reconstruction of SST (1854–1997). *J. Climate*, **17**, 2466–2477.
- Solomon, S., and Coauthors, 2007: *Climate Change 2007: The Physical Science Basis*. Cambridge University Press, 996 pp.
- Taylor, K. E., R. J. Stouffer, and G. A. Meehl, 2009: A summary of the CMIP5 experimental design. WCRP CMIP Rep., 30 pp. [Available online at [http://cmip-pcmdi.llnl.gov/cmip5/docs/Taylor\\_CMIP5\\_dec31.pdf](http://cmip-pcmdi.llnl.gov/cmip5/docs/Taylor_CMIP5_dec31.pdf).]
- , —, and —, 2012: An overview of CMIP5 and the experiment design. *Bull. Amer. Meteor. Soc.*, **93**, 485–498.
- Timmermann, A., 2003: Decadal ENSO amplitude modulations: A nonlinear paradigm. *Global Planet. Change*, **37**, 135–156.
- , and Coauthors, 1999: Increased El Niño frequency in a climate model forced by future greenhouse warming. *Nature*, **393**, 694–697.
- Trenberth, K. E., and T. J. Hoar, 1996: The 1990–1995 El Niño–Southern Oscillation event: Longest on record. *Geophys. Res. Lett.*, **23**, 57–60.
- Vecchi, G. A., A. Clement, and B. J. Soden, 2008: Examining the tropical Pacific’s response to global warming. *Eos, Trans. Amer. Geophys. Union*, **89**, 81, doi:10.1029/2008EO090002.
- Xie, S.-P., C. Deser, G. A. Vecchi, J. Ma, H. Teng, and A. T. Wittenberg, 2010: Global warming pattern formation: Sea surface temperature and rainfall. *J. Climate*, **23**, 966–986.
- Yeh, S.-W., and B. P. Kirtman, 2004: Tropical Pacific decadal variability and ENSO amplitude modulation in a CGCM. *J. Geophys. Res.*, **109**, C11009, doi:10.1029/2004JC002442.
- , J.-S. Kug, B. Dewitte, M.-H. Kwon, B. P. Kirtman, and F.-F. Jin, 2009: El Niño in a changing climate. *Nature*, **461**, 511–514.